

Supporting Information

Unveiling the role of upper excited states in the photochemistry and laser performance of *anti*-B₁₈H₂₂.

Luis Cerdán,^{1} Antonio Francés-Monerris,^{2,3} Daniel Roca-Sanjuán,^{4*} Jonathan Bould,⁵ Jiří Dolanský,⁵ Marcel Fuciman,⁶ and Michael G. S. Londesborough^{5*}*

¹ Institute of Physical Chemistry “Rocasolano”, Consejo Superior de Investigaciones Científicas (CSIC), C/ Serrano 119, 28006, Madrid, Spain

² Université de Lorraine and CNRS, LPCT, F-54000 Nancy, France

³ Departament de Química Física, Universitat de València, Dr. Moliner 50, 46100 Burjassot, Spain

⁴ Institut de Ciència Molecular, Universitat de València, P.O.Box 22085, 46010 Valencia - Spain

⁵ Institute of Inorganic Chemistry of the Czech Academy of Sciences, 250 68 Husinec-Řež, Czech Republic

⁶ Institute of Physics, Faculty of Science, University of South Bohemia, Branišovská 1760, 370 05 České Budějovice, Czech Republic

**lcerdanphd@gmail.com; *Daniel.Roca@uv.es; *michaell@iic.cas.cz*

Section S1. Calculation of Excited State Absorption (ESA) cross section at the pump wavelength.

Section S2. Reconstruction of cross section spectra from oscillator strengths and transition energies.

Table S1. Vertical absorption and emission energies (ν_{if}) (in eV and nm) and associated oscillator strengths (f_{if}) between states S_i and S_j of *anti*-B₁₈H₂₂ at the S_0 and S_1 minimum geometry determined with two different methods (CASPT2 and MS-CASPT2).

Figure S1. ¹¹B (above) and ¹H (below) NMR spectra of white precipitate from cuvette wall formed after continual 355 nm laser excitation.

Figure S2. Experimental set-ups for the intensity dependent transmission (a) and the long-irradiation (b) experiments

Figure S3. Photodegradation samples photographed before opening under visible white light

Figure S4. Direct comparison of samples 0mins (left) and 210mins (right).

Figure S5. Samples 0mins, 150mins and 210mins in cyclohexane solution in quartz NMR tubes under UV lamp

Figure S6. ¹¹B-¹H NMR spectrum of reference sample 0mins(0 MJ)

Figure S7. $^{11}\text{B}\{-^1\text{H}\}$ NMR spectrum of sample 15mins(0.11 MJ)
Figure S8. $^{11}\text{B}\{-^1\text{H}\}$ NMR spectrum of sample 30mins(0.22 MJ)
Figure S9. $^{11}\text{B}\{-^1\text{H}\}$ NMR spectrum of sample 60mins(0.43 MJ)
Figure S10. $^{11}\text{B}\{-^1\text{H}\}$ NMR spectrum of sample 120mins(0.86 MJ)
Figure S11. $^{11}\text{B}\{-^1\text{H}\}$ NMR spectrum of sample 210mins(1.51 MJ)
Figure S12. $^{11}\text{B}\{-^1\text{H}\}$ NMR spectrum of sample 150mins(0.11 MJ)
Figure S13. Full (top) and expanded (bottom) mass spectrum 210m (1.15 MJ) sample of *anti*- $\text{B}_{18}\text{H}_{22}$.
Figure S14. CASSCF natural orbitals corresponding to the dominant excitations (configuration state functions) that characterise the $\text{S}_1(\text{a})$, $\text{S}_8(\text{b})$, $\text{S}_{11}(\text{c})$, and $\text{S}_{12}(\text{d})$ states.
Figure S15. $^{11}\text{B}\{-^1\text{H}\}$ spectrum of *anti*- $\text{B}_{18}\text{H}_{22}$ sample irradiated for a period of 270 minutes
Figure S16. Mass spectrum of of *anti*- $\text{B}_{18}\text{H}_{22}$ sample irradiated for a period of 270 minutes
Figure S17. Reference (left-hand side) and 270 minute irradiated (right-hand side) samples of *anti*- $\text{B}_{18}\text{H}_{22}$ in *c*-hexane under UV lamp irradiation.

Section S1. Calculation of Excited State Absorption (ESA) cross section at the pump wavelength.

We first assume that a Gaussian pulse with a pulse full width half maximum τ_p (7 ns) is travelling downwards (Z-axis) and impinges on the upper surface of the solution at $Z=0$ (Equation S1). The photon flux (#photons $s^{-1} cm^{-2}$) in this point will follow the expression:

$$I_p(z=0, t) = I_p^0 e^{-\frac{(t-t_0)^2}{(\tau_p/2)^2} \log 2} \quad (S1)$$

As it propagates within an absorptive medium of length L , it will be absorbed by the populations of the ground state (N_0) and the first (N_1) and upper excited states (N_N). Thus, the pump photon flux follows the spatio-temporal equation:

$$\begin{aligned} \frac{dI_p(z, t)}{dz} = \frac{n}{c} \frac{\partial I_p(z, t)}{\partial t} + \frac{\partial I_p(z, t)}{\partial z} = \\ -\sigma_{0p} N_0(z, t) I_p(z, t) - \sigma_{1p} N_1(z, t) I_p(z, t) - \sigma_{Np} N_N(z, t) I_p(z, t) \end{aligned} \quad (S2)$$

where n is the medium refractive index (1.43), c the speed of light in vacuum, σ_{0p} , σ_{1p} and σ_{Np} are the ground (S_0) and S_1 , S_N excited-state absorption cross-sections at the pump wavelength, and N_0 , N_1 and N_N are the volume density of molecules in the S_0 , S_1 , and S_N states. The populations N_i (with $i=0,1,N$) evolve in time and space as:

$$\begin{aligned} \frac{dN_N(z, t)}{dt} &= \sigma_{1p} N_1(z, t) I_p(z, t) - \frac{N_N(z, t)}{\tau_N} - \sigma_{Np} N_N(z, t) I_p(z, t); \\ \frac{dN_1(z, t)}{dt} &= \sigma_{0p} N_0(z, t) I_p(z, t) - \frac{N_1(z, t)}{\tau} - \sigma_{1p} N_1(z, t) I_p(z, t) + \frac{N_N(z, t)}{\tau_N}; \\ N_d &= N_0(z, t) + N_1(z, t) + N_N(z, t) \end{aligned} \quad (S3)$$

where τ_N and τ are the life-times of the upper and first excited states, respectively. N_d is the volume density of active molecules in the solution. In the present approach, we will assume, as a reasonable approximation, that the pump photon flux is not absorbed by upper excited states S_N , and therefore $\sigma_{Np} = 0$. This implies that, effectively, the whole of the excited state absorption takes place in the first excited state S_1 . The population and intensity propagation equations (S2) and (S3) then simplifies to:

$$\begin{aligned} \frac{dI_p(z, t)}{dz} &= \frac{n}{c} \frac{\partial I_p(z, t)}{\partial t} + \frac{\partial I_p(z, t)}{\partial z} = -\sigma_{0p} N_0(z, t) I_p(z, t) - \sigma_{1p} N_1(z, t) I_p(z, t) \\ \frac{dN_N(z, t)}{dt} &= \sigma_{1p} N_1(z, t) I_p(z, t) - \frac{N_N(z, t)}{\tau_N}; \\ \frac{dN_1(z, t)}{dt} &= \sigma_{0p} N_0(z, t) I_p(z, t) - \frac{N_1(z, t)}{\tau} - \sigma_{1p} N_1(z, t) I_p(z, t) + \frac{N_N(z, t)}{\tau_N}; \\ N_d &= N_0(z, t) + N_1(z, t) + N_N(z, t) \end{aligned} \quad (S4)$$

Numerically solving the system of coupled differential equations (S4) with boundary conditions (S1), allows obtaining the pump photon flux exiting the medium $I_p(z=L, t)$. Thus, the numerically computed value of transmission is given by:

$$T = 100\% \frac{\int I_p(z=L, t) dt}{\int I_p(z=0, t) dt} \quad (\text{S5})$$

To compute the proportion of pump photons that are absorbed due to Ground State Absorption (GSA) or Excited State Absorption (ESA), the following propagation equations are solved in parallel with the system of eqs. (S4):

$$\begin{aligned} \frac{dI_{p,GSA}(z, t)}{dz} &= \frac{n}{c} \frac{\partial I_{p,GSA}(z, t)}{\partial t} + \frac{\partial I_{p,GSA}(z, t)}{\partial z} = -\sigma_{0p} N_0(z, t) I_{p,GSA}(z, t) \\ \frac{dI_{p,ESA}(z, t)}{dz} &= \frac{n}{c} \frac{\partial I_{p,ESA}(z, t)}{\partial t} + \frac{\partial I_{p,ESA}(z, t)}{\partial z} = -\sigma_{1p} N_1(z, t) I_{p,ESA}(z, t) \end{aligned} \quad (\text{S6})$$

using the values of N_0 and N_1 updated while solving the system of eqs. (S4). The proportion of photons absorbed due to GSA or ESA is then given by:

$$\begin{aligned} \alpha_{GSA} &= 1 - \frac{\int I_{p,GSA}(z=L, t) dt}{\int I_{p,GSA}(z=0, t) dt} \\ \alpha_{ESA} &= 1 - \frac{\int I_{p,ESA}(z=L, t) dt}{\int I_{p,ESA}(z=0, t) dt} \end{aligned} \quad (\text{S7})$$

It is easy to see that the total amount of absorbed pump photons ($\alpha = 1 - T/100$) must be the sum of the amount of photons absorbed by GSA and ESA, *i.e.*, $\alpha = \alpha_{GSA} + \alpha_{ESA}$. Thus, the percentage of absorbed photons that goes into ESA, ρ_{ESA} , is calculated as:

$$\rho_{ESA} = \frac{\alpha_{ESA}}{\alpha_{GSA} + \alpha_{ESA}} \quad (\text{S8})$$

Section S2. Reconstruction of cross section spectra from oscillator strengths and transition energies.

Computing the transitions band shape in a formal way would involve determining the vibronic couplings between all the electronic states. Even though for the lowest-lying states (S_0 and S_1) this would be reasonable to do, for upper excited states, with their strong multiconfigurational character, large anharmonicity and many near-degeneracies, accurate and reliable computations of the vibronic couplings within the CASSCF/(MS-)CASPT2 approach become prohibitive. Accordingly, in the present work, we opted for a simpler, but standard, approach^{S1,S2} based on assigning each computed transition with a Gaussian function the proportionality factor of which is determined by the oscillator strength and transition energy. In an ideal case, each transition would have to be assigned its own line-width, but it is qualitatively sufficient to assign the same line-width to all transitions. This line-width $\Delta\nu$ is usually chosen to replicate the experimentally available absorption bands line-widths. To get an improved prediction of the bands line-shapes, nuclear sampling of the ground-state Franck-Condon minimum could be done with a semi-classical Wigner distribution based on the frequencies and subsequently convolving each point of the distribution with Gaussian functions.^{S3} Nevertheless, since experimental spectroscopic data is available in our study, the single electronic transition at the equilibrium structures of S_0 and S_1 , and correlation to the measured spectra, is sufficient for the objectives of this work, avoiding very high computational demands that would be required in the relatively large-size of the octadecaborane molecule that we study herein.

The proportionality factor is computed as follows. The oscillator strength for an electronic transition between an initial state i and a final state f (f_{if}) and the molar extinction coefficient ϵ_{ij} spectrum (in $M^{-1} cm^{-1}$) of a given transition centred at an energy ν_{if} are related through the common expression:^{S4}

$$f_{if} = 8065.5 \cdot 4.32 \times 10^{-9} F(n, \nu_{if}) \int \epsilon_{ij} d\nu \quad (S9)$$

The leading 8065.5 factor has been included to take into account that the energy ν is expressed in eV instead of cm^{-1} , as is usually done. $F(n, \nu_{if})$ is the local field factor that takes the solvent effects into account. In the Onsager real cavity approximation^{S5} $F(n, \nu_{if}) = (2n(\nu_{if})^2 + 1)^2 / (9n(\nu_{if})^3)$, with $n(\nu_{if})$ being the solvent refractive index at transition energy ν_{if} . The molar extinction coefficient, ϵ_{if} , is defined as a Gaussian function:

$$\epsilon_{ij}(\nu) = \frac{\epsilon_{max}}{\sqrt{2\pi}\Delta\nu/2.3548} e^{-\frac{(\nu - \nu_{if})^2}{2(\Delta\nu/2.3548)^2}} \quad (S10)$$

so that $\int \epsilon_{ij} d\nu = \epsilon_{max}$. Substituting (S10) into (S9), and solving for ϵ_{max} , leads to:

$$\epsilon_{max} = \frac{f_{if}}{8065.5 \cdot 4.32 \times 10^{-9} F(n, \nu_{if})} \quad (S11)$$

On the other hand, the absorption cross section, $\sigma_{if}(\nu)$, (in cm^2) and the ϵ_{if} , (in $M^{-1} cm^{-1}$) are related as:

$$\sigma_{ij}(\nu) = \ln(10) \cdot 1000 \frac{\varepsilon_{ij}(\nu)}{N_A} \quad (\text{S12})$$

where N_A is Avogadro's number. Substituting (S11) into (S10) and the resulting expression into (S12), leads to the absorption cross section of each transition:

$$\sigma_{ij}(\nu) = \frac{\ln(10) \cdot 1000}{N_A \sqrt{2\pi} \Delta\nu / 2.3548} \frac{f_{ij}}{8065.4 \cdot 4.32 \times 10^{-9} F(n, \nu_{ij})} e^{-\frac{(\nu - \nu_{ij})^2}{2(\Delta\nu / 2.3548)^2}} \quad (\text{S13})$$

The absorption spectrum of the initial state i is thus obtained summing up the individual contributions of each transition:

$$\sigma_i(\nu) = \sum_j \sigma_{ij}(\nu) = \sum_j 1.03 \times 10^{-16} \frac{f_{ij}}{F(n, \nu_{ij}) \Delta\nu} e^{-\frac{(\nu - \nu_{ij})^2}{2(\Delta\nu / 2.3548)^2}} \quad (\text{S14})$$

Equation (S14) thus constructs the cross-section spectrum from oscillator strengths and transition energies. The indexes i and f run as follows for each type of spectrum determined in this work: for GSA, $i = 0$ and $f = 1 \dots N$, and for ESA, $i = 1$ and $f = 2 \dots N_{tot}$, where N_{tot} is the total number of electronic states considered.

References

- S1. R. Rürger, E. van Lenthe, Y. Lu, J. Frenzel, T. Heine and L. Visscher, "Efficient Calculation of Electronic Absorption Spectra by Means of Intensity-Selected Time-Dependent Density Functional Tight Binding," *J. Chem. Theory Comput.* 11, 157-167 (2015).
- S2. E. F. Oliveira, J. Shi, F. C. Lavarda, L. Lürer, B. Milián-Medina, and J. Gierschner, "Excited state absorption spectra of dissolved and aggregated distyrylbenzene: A TD-DFT state and vibronic analysis" *J. Chem. Phys.* 147, 034903 (2017).
- S3. E. Wigner, *Phys. Rev.* 40 (1932) 749.
- S4. J. R. Lakowicz, *Principles of Fluorescence Spectroscopy* 3rd Ed. (Springer, 2006).
- S5. K. Dolgaleva and R. W. Boyd, "Local-field effects in nanostructured photonic materials," *Adv. Opt. Photon.* 4, 1-77 (2012).

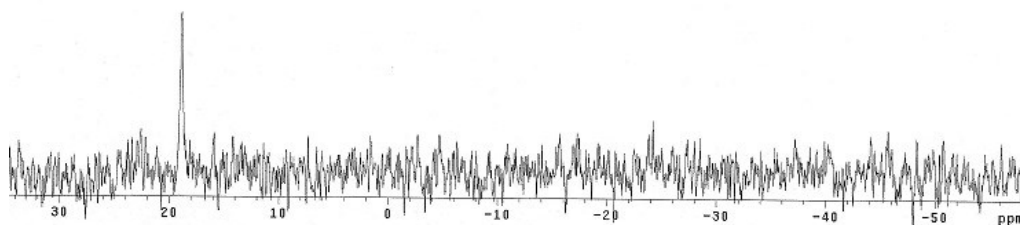
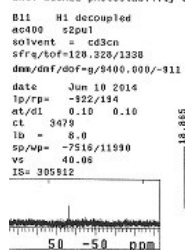
Table S1. Vertical absorption and emission energies (ν_{if}) (in eV and nm) and associated oscillator strengths (f_{if}) between states S_i and S_j of *anti*-B₁₈H₂₂ at the S_0 and S_1 minimum geometry determined with two different methods (CASPT2 and MS- CASPT2).

Transition	CASPT2			MS-CASPT2		
	ν_{if} (eV)	ν_{if} (nm)	f_{if}	ν_{if} (eV)	ν_{if} (nm)	f_{if}
absorption at the S_0 -minimum geometry (GSA)						
$S_0 \rightarrow S_1$	3.93	315	0.2917	3.93	315	0.3136
$S_0 \rightarrow S_2$	5.00	248	0.1709	4.99	248	0.1676
$S_0 \rightarrow S_3$	5.03	246	0.0000	5.02	247	0.0000
$S_0 \rightarrow S_4$	5.35	232	0.0000	5.33	233	0.0000
$S_0 \rightarrow S_5$	5.43	228	0.0000	5.42	229	0.0000
$S_0 \rightarrow S_6$	5.52	225	0.0390	5.54	224	0.0283
$S_0 \rightarrow S_7$	5.76	215	0.0000	5.80	214	0.0000
absorption at the S_1 -minimum geometry (ESA)						
$S_1 \rightarrow S_2$	1.31	944	0.0421	1.25	992	0.0523
$S_1 \rightarrow S_3$	1.54	808	0.0000	1.51	824	0.0000
$S_1 \rightarrow S_4$	1.63	763	0.0000	1.64	757	0.1035
$S_1 \rightarrow S_5$	1.71	725	0.0766	1.68	740	0.0000
$S_1 \rightarrow S_6$	1.77	700	0.0191	1.89	655	0.0665
$S_1 \rightarrow S_7$	2.17	570	0.0271	2.22	560	0.0030
$S_1 \rightarrow S_8$	2.60	476	0.3509	2.67	464	0.3658
$S_1 \rightarrow S_9$	3.02	410	0.0000	3.03	409	0.0000
$S_1 \rightarrow S_{10}$	3.25	382	0.0000	3.29	376	0.0000
$S_1 \rightarrow S_{11}$	3.33	373	0.0902	3.39	366	0.0145
$S_1 \rightarrow S_{12}$	3.61	344	0.0304	3.66	339	0.0048
$S_1 \rightarrow S_{13}$	3.96	313	0.0000	3.95	314	0.0000
$S_1 \rightarrow S_{14}$	4.10	303	0.0000	4.11	302	0.0000
$S_1 \rightarrow S_{15}$	4.20	295	0.1090	4.17	297	0.0991
$S_1 \rightarrow S_{16}$	4.22	294	0.0000	4.40	282	0.0000
$S_1 \rightarrow S_{17}$	4.41	281	0.0596	4.52	275	0.0279
$S_1 \rightarrow S_{18}$	4.53	274	0.0530	4.68	265	0.0000

$S_1 \rightarrow S_{19}$	4.54	273	0.0130	4.71	263	0.0018
emission at the S_1 minimum geometry (SE)						
$S_1 \rightarrow S_0$	3.00	413	0.3279	2.97	417	0.4356

Figure S1. ^{11}B (above) and ^1H (below) NMR spectra of white precipitate from cuvette wall formed after continual 355 nm laser excitation.

anti-B18H22 photostability experiment - white spots on side of cuvette



```

dmn/dmf/dof=g/9930.000/965

```

```

date Jun 10 2014
lp/rp= -316/-129
at/d1 0.15 4.00
ct 32
gf = 0.090000
gfs = 0.001000
sp/wp= -711/3050
vs 135.40
IS= 11166

```

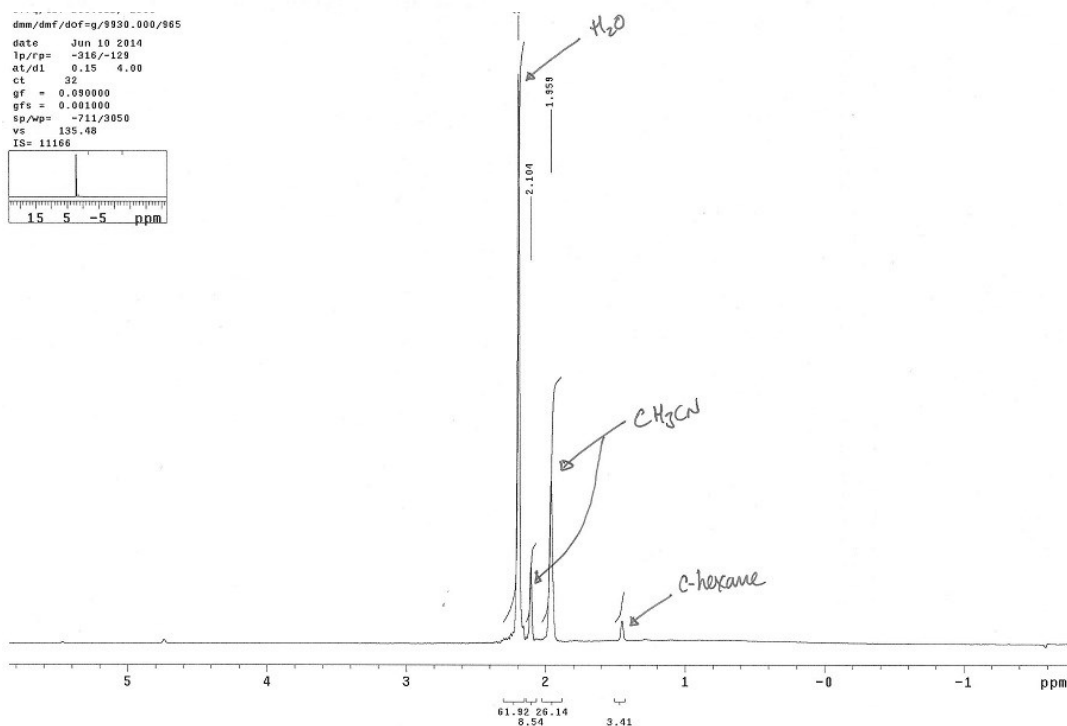
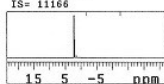


Figure S2: Experimental set-ups for the intensity dependent transmission (a) and the long-irradiation (b) experiments.

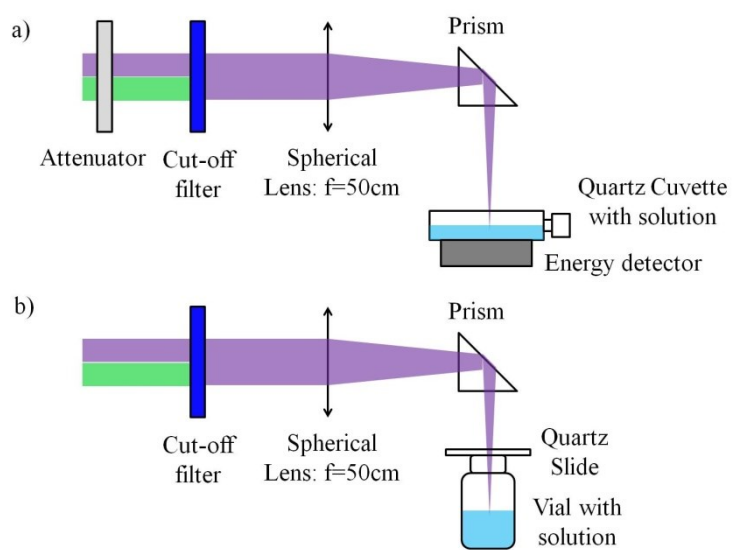


Figure S3. Photodegradation samples photographed before opening under visible white light

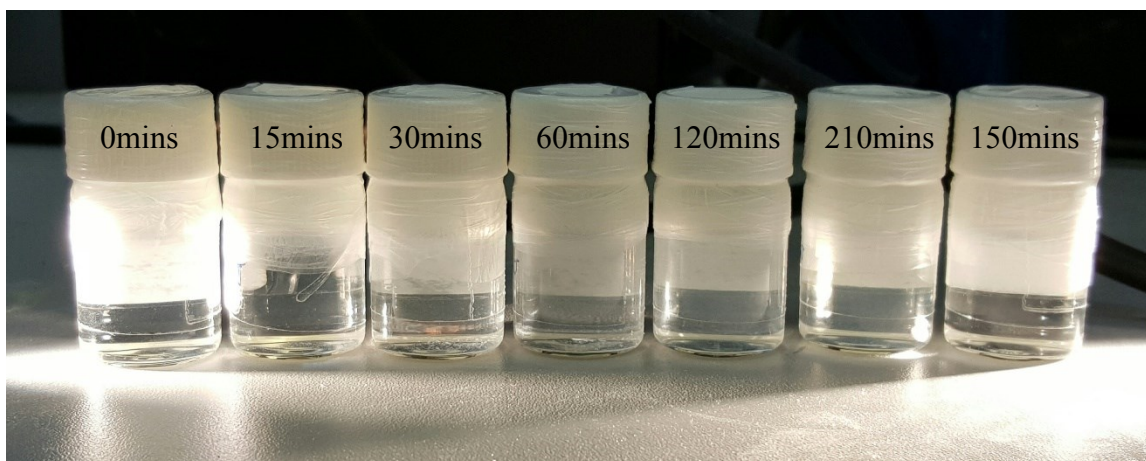


Figure S4. Direct comparison of samples 210mins (left) and 0mins (right). Note the slight yellowish hue and traces of white precipitate at the bottom of the left-hand vial.

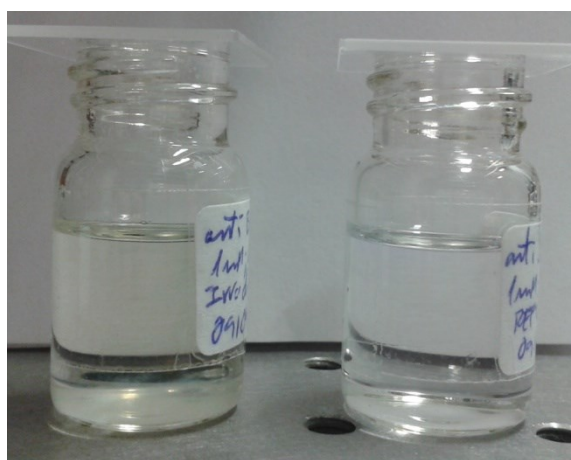


Figure S5. Samples 0mins, 150mins and 210mins in cyclohexane solution in quartz NMR tubes under UV lamp

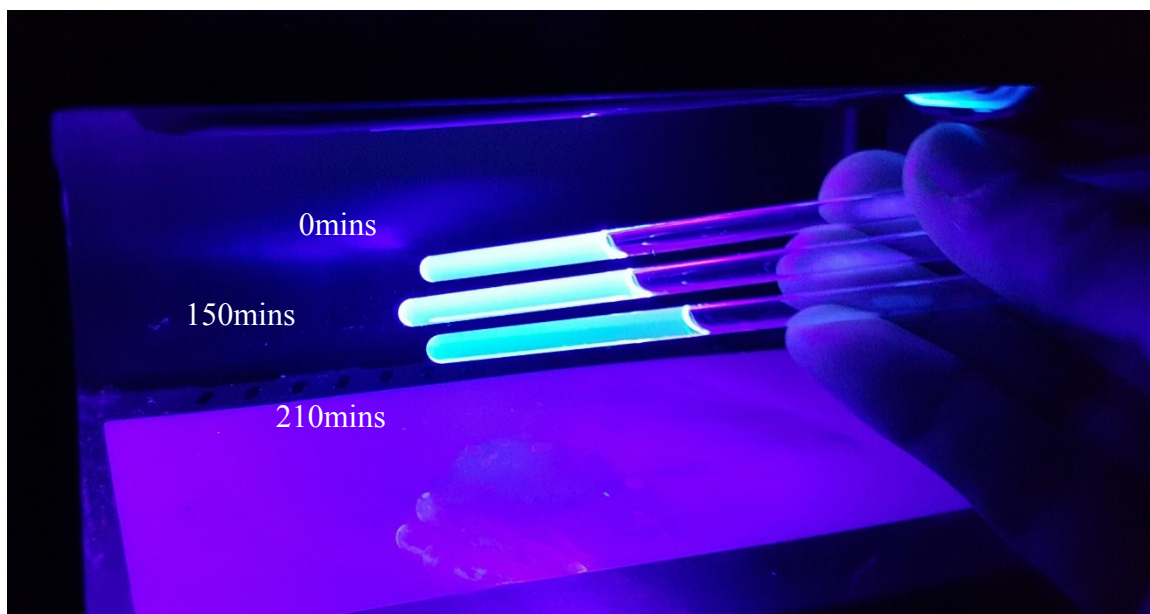


Figure S6. $^{11}\text{B}\{-^1\text{H}\}$ NMR spectrum of reference sample 0mins(0 MJ)

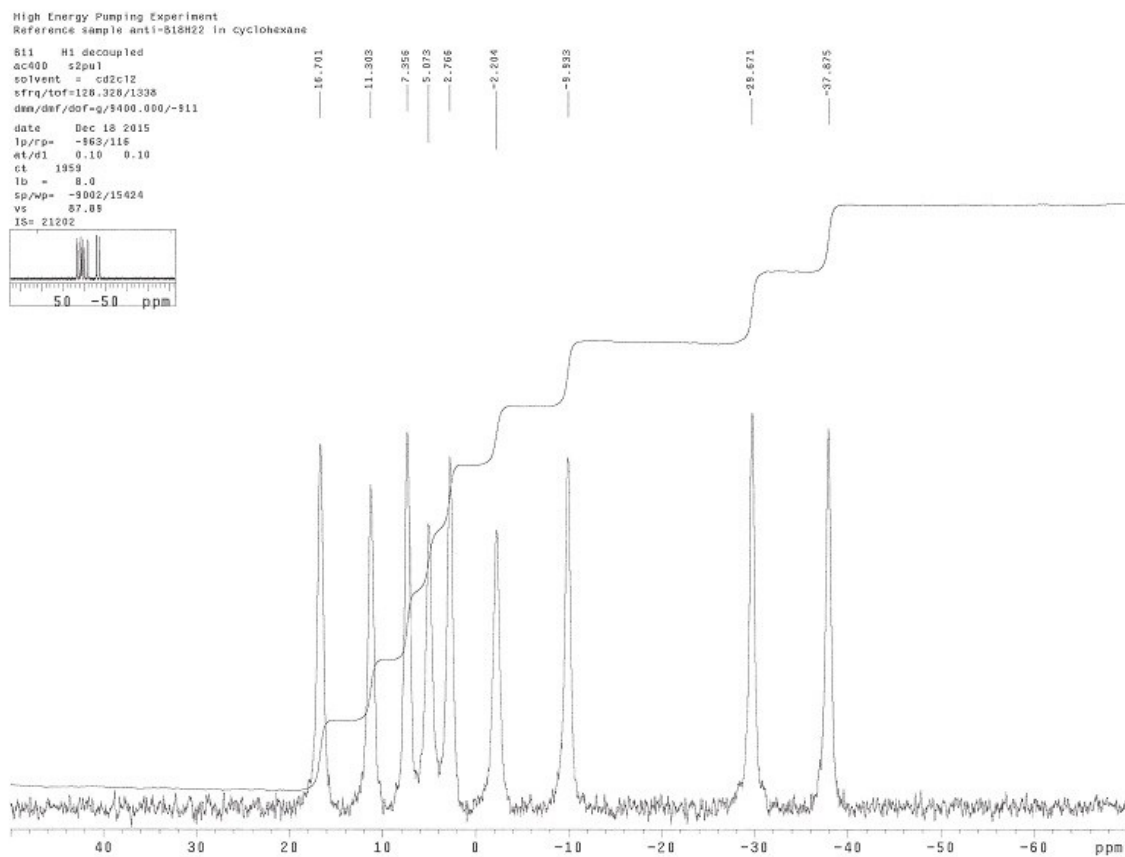


Figure S7. $^{11}\text{B}\{-^1\text{H}\}$ NMR spectrum of sample 15mins(0.11 MJ)

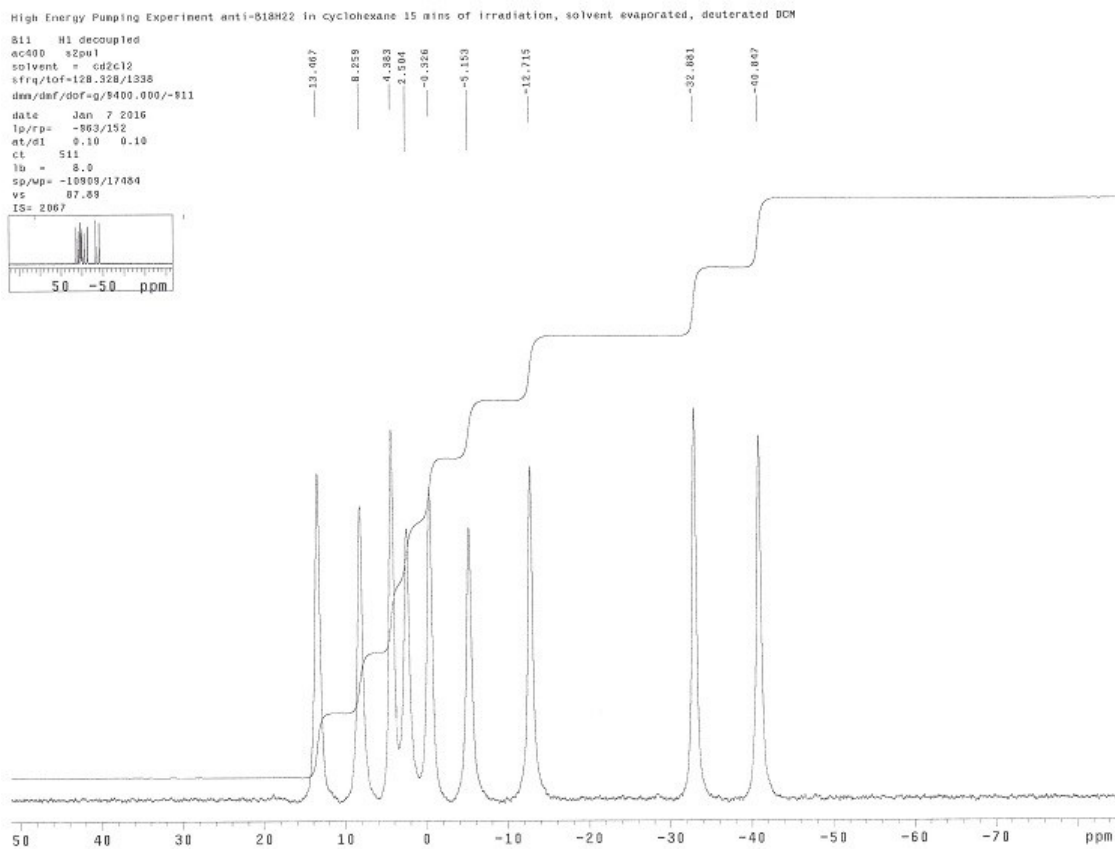
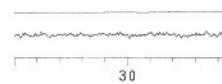


Figure S8. $^{11}\text{B}\{-^1\text{H}\}$ NMR spectrum of sample 30mins(0.22 MJ)



Figure S9. $^{11}\text{B}\{-^1\text{H}\}$ NMR spectrum of sample 60mins(0.43 MJ)



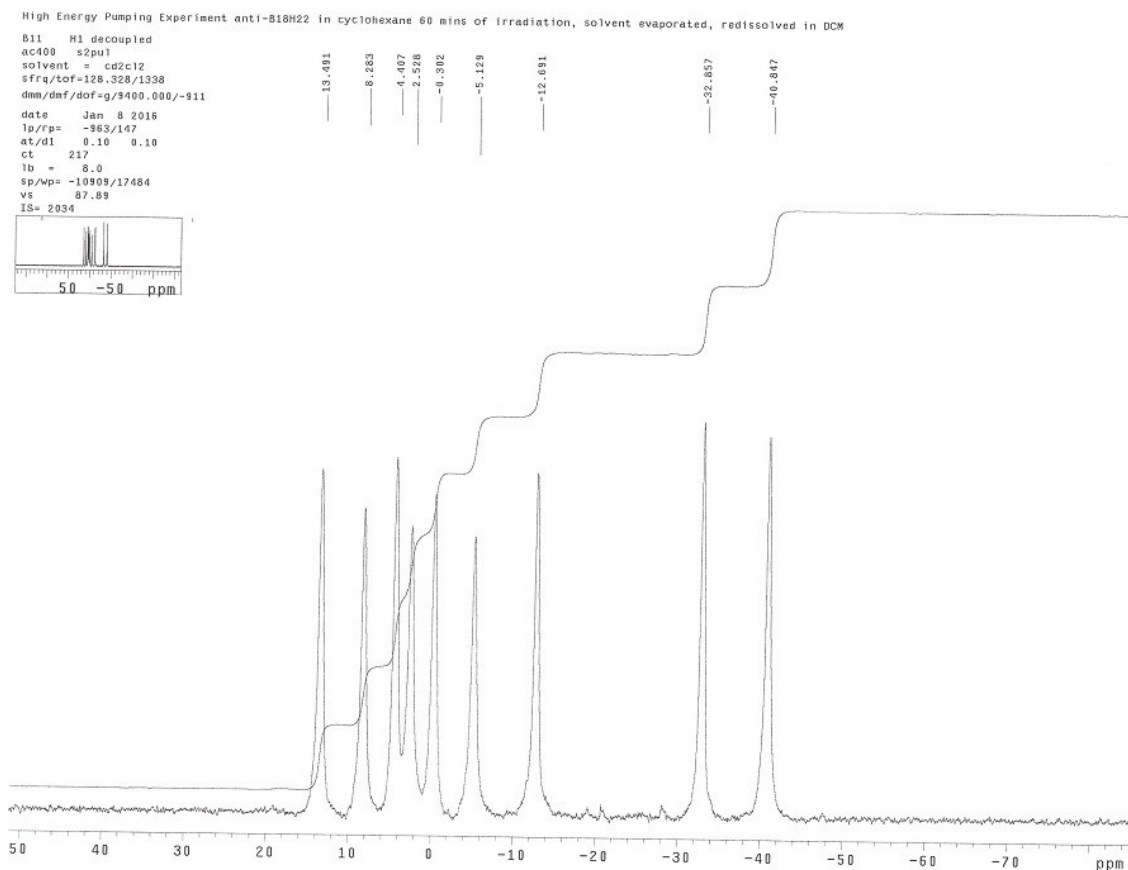


Figure S10. $^{11}\text{B}-\{^1\text{H}\}$ NMR spectrum of sample 120mins(0.86 MJ)

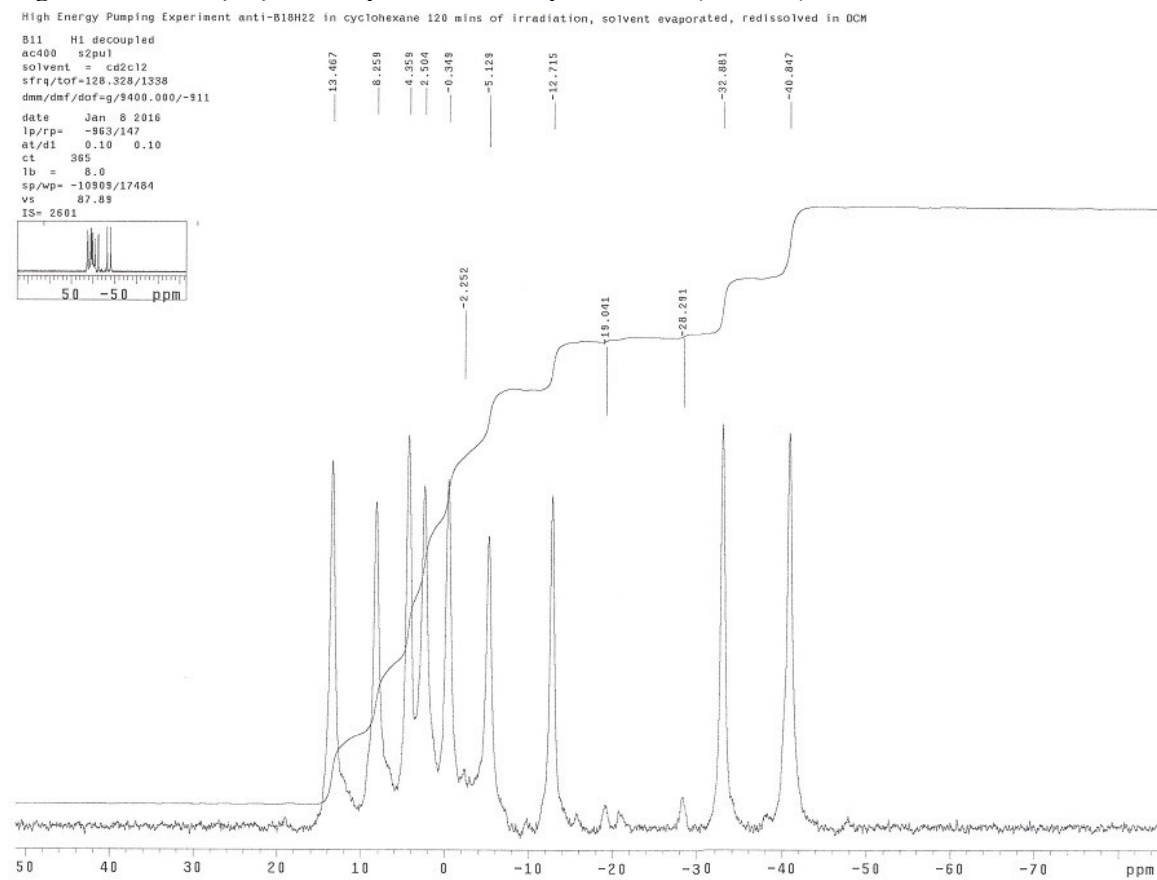


Figure S11. $^{11}\text{B}-\{^1\text{H}\}$ NMR spectrum of sample 210mins(1.51 MJ)

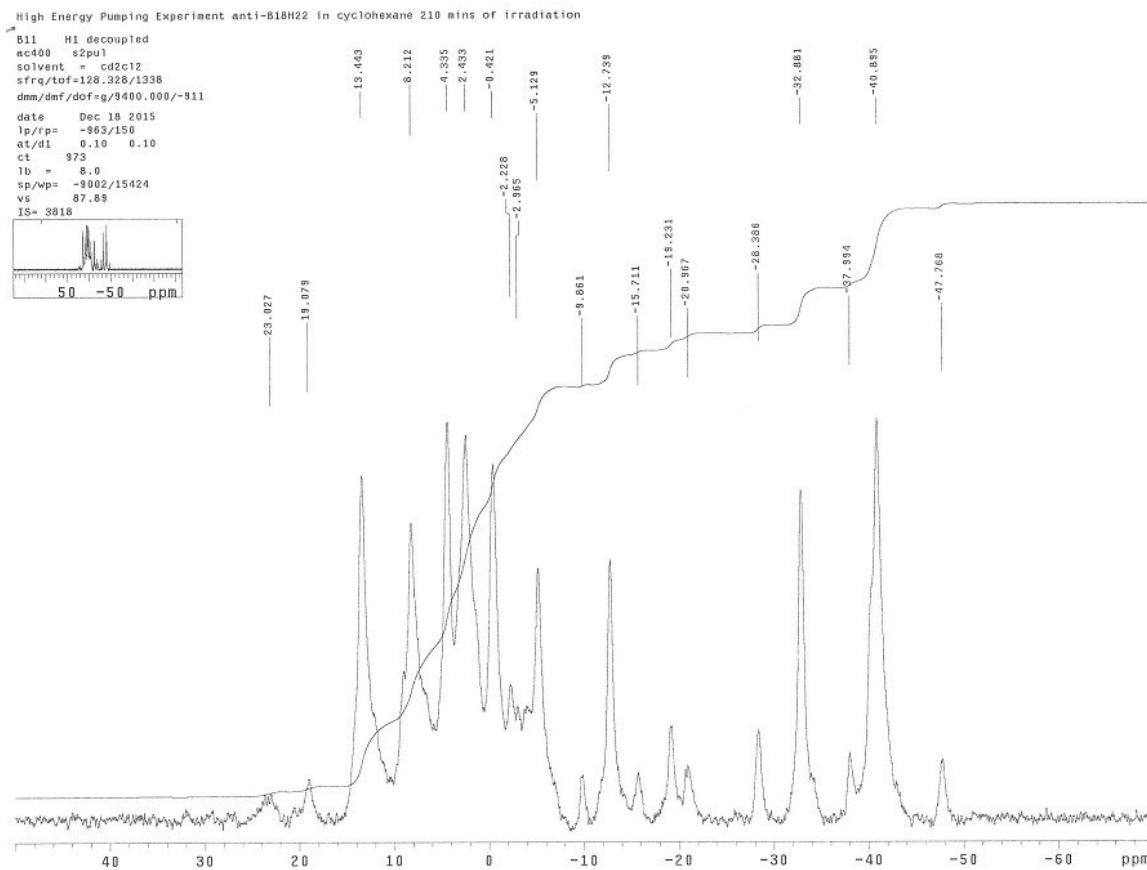


Figure S12. $^{11}\text{B}\{-^1\text{H}\}$ NMR spectrum of sample 150mins(0.11 MJ)

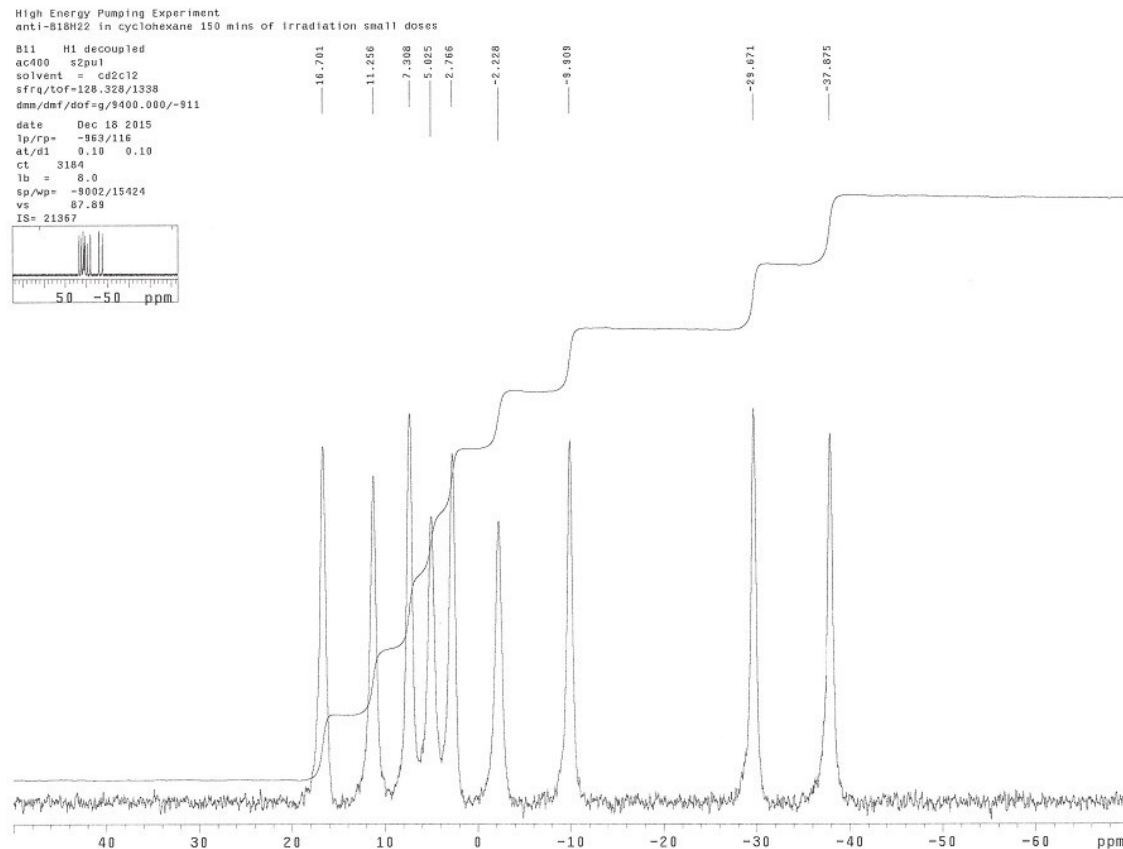
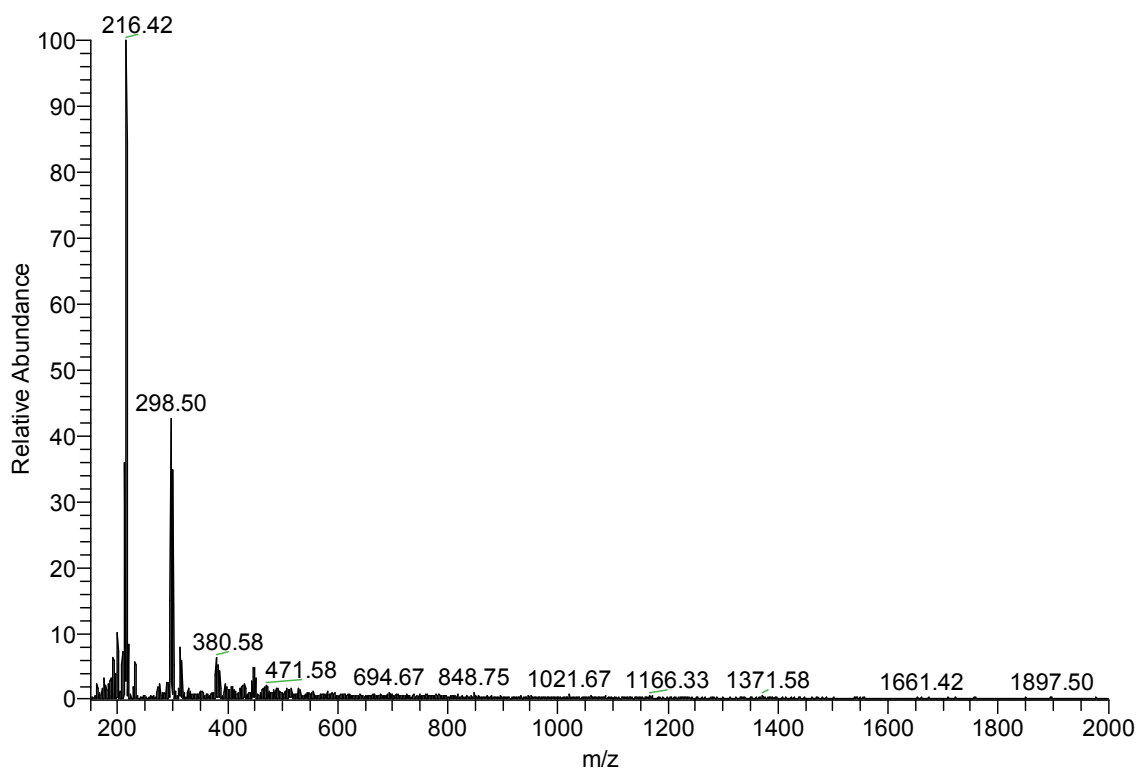


Figure S13. Full (top) and expanded (bottom) mass spectrum 210m (1.15 MJ) sample of *anti*-B₁₈H₂₂.



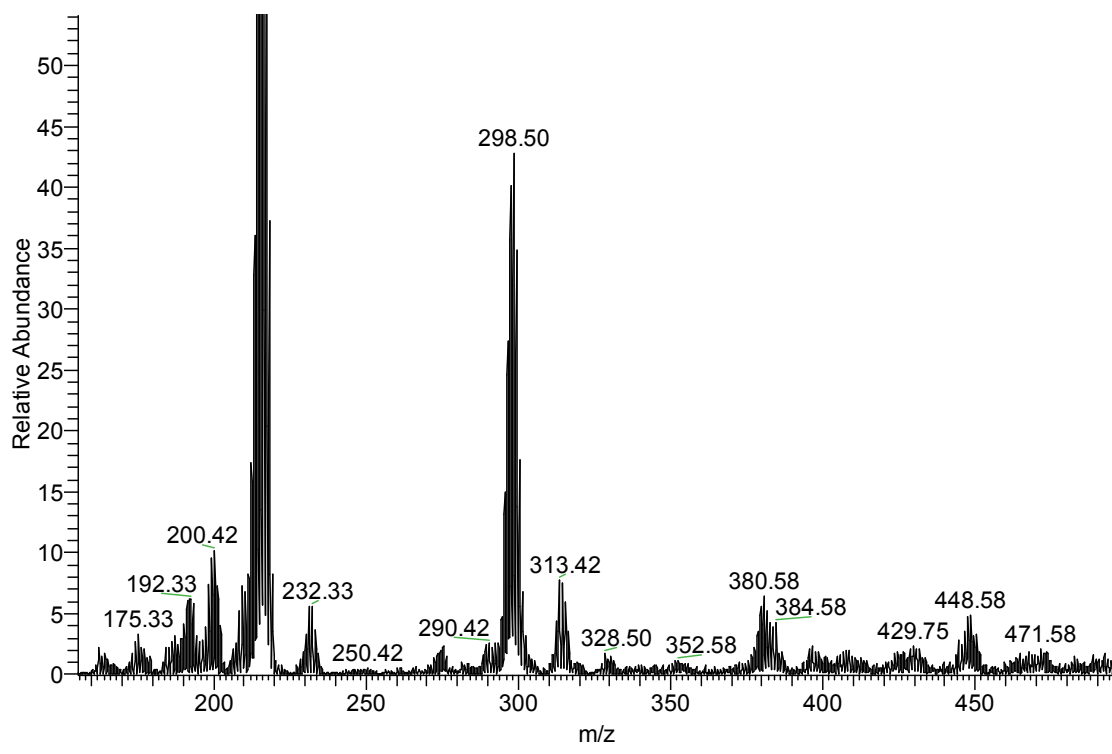


Figure S14. CASSCF natural orbitals corresponding to the dominant excitations (configuration state functions) that characterise the S_1 (a), S_8 (b), S_{11} (c), and S_{12} (d) states. Dotted yellow lines indicate the bonds with antibonding character, and **B** refers to the *conjuncto* boron atoms that are shared by the molecule's two subclusters.

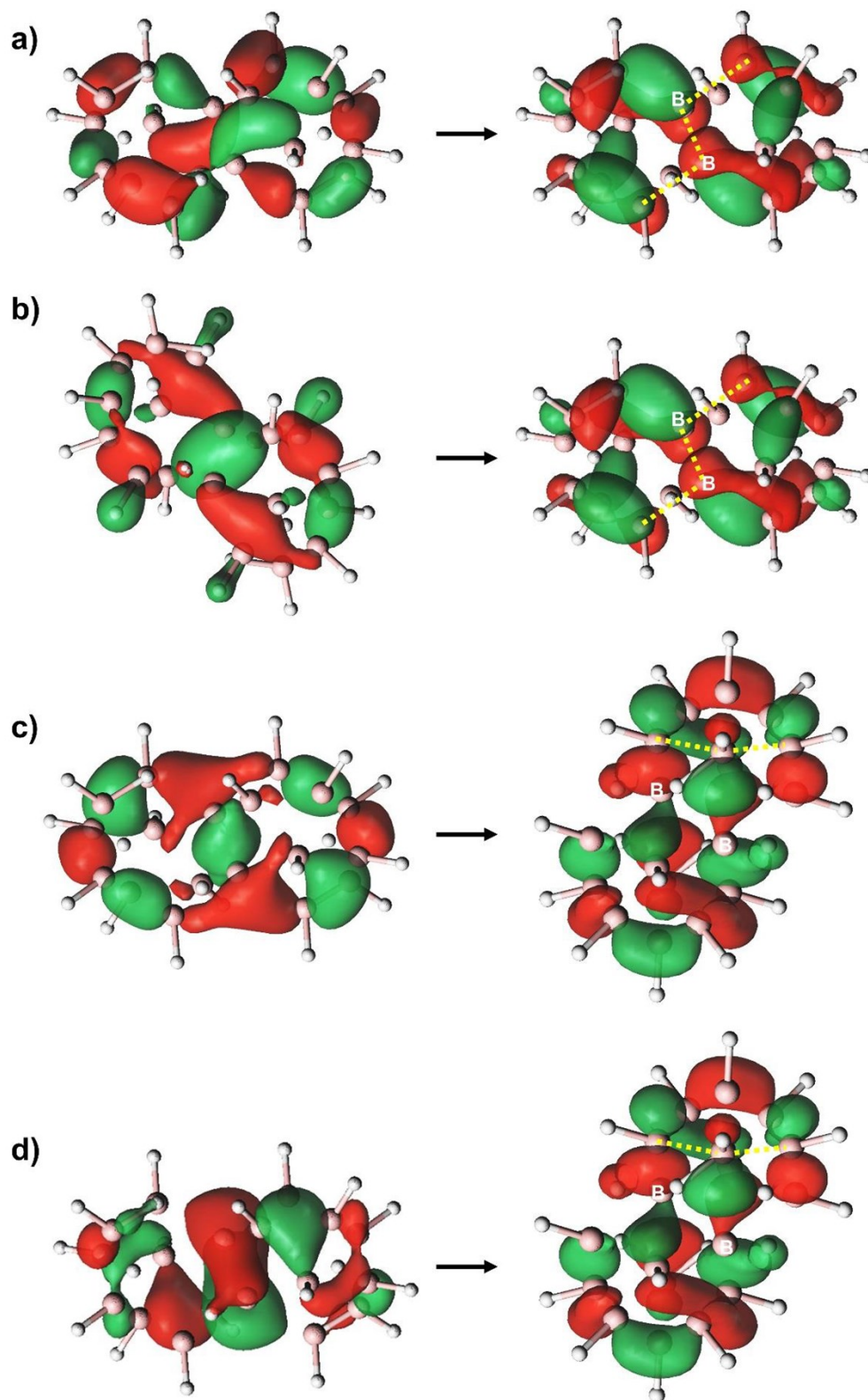


Figure S15. $^{11}\text{B}\{-^1\text{H}\}$ spectrum of *anti*- $\text{B}_{18}\text{H}_{22}$ sample irradiated for a period of 270 minutes

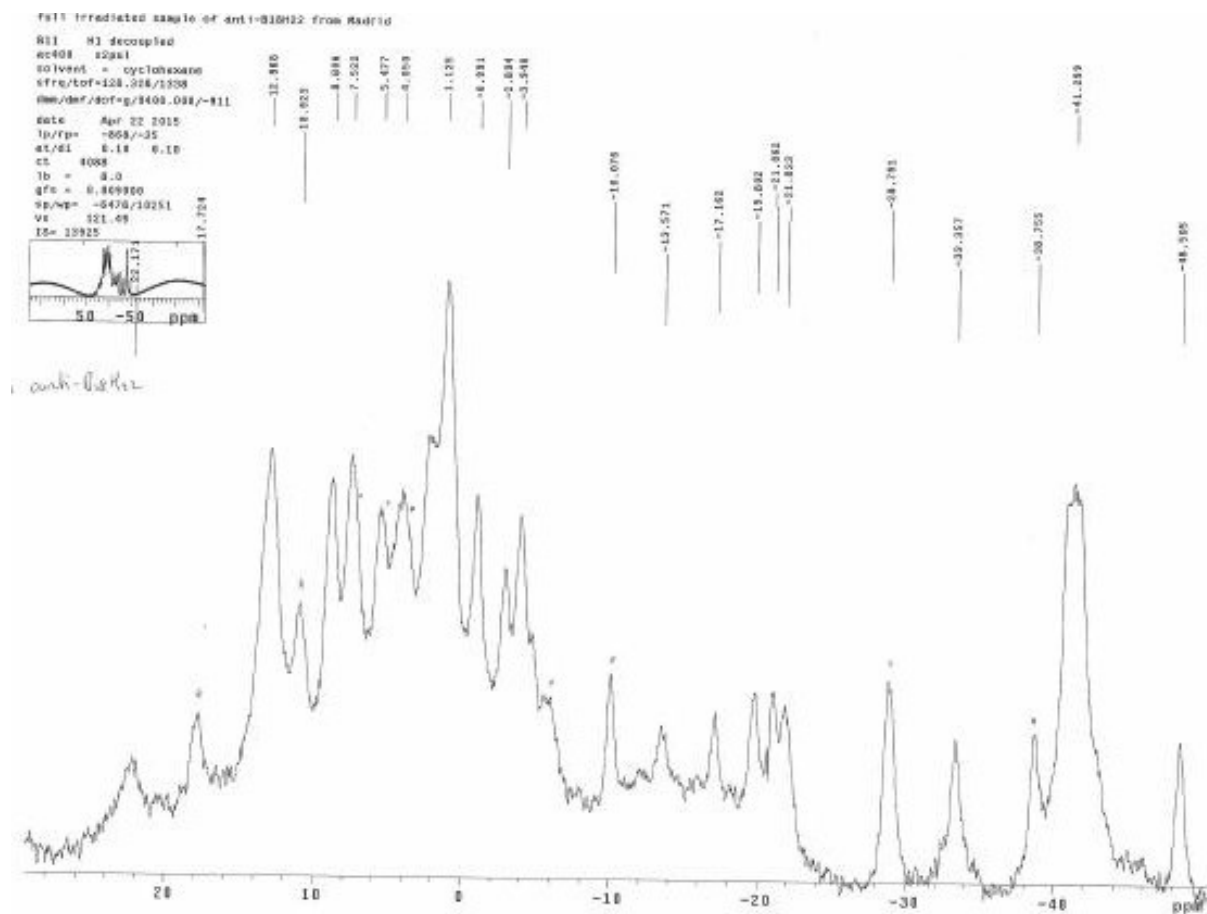


Figure S16. Mass spectrum of of *anti*-B₁₈H₂₂ sample irradiated for a period of 270 minutes

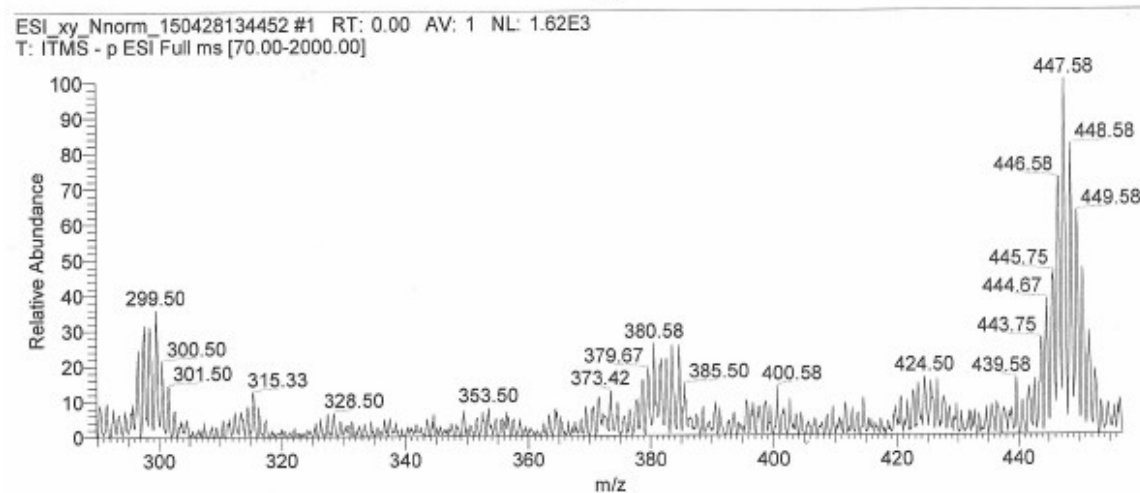
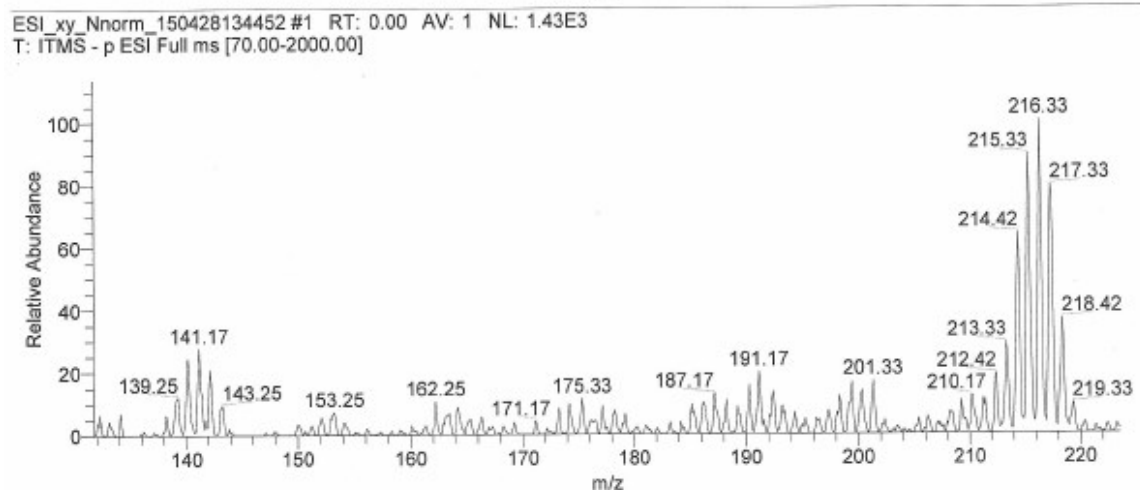
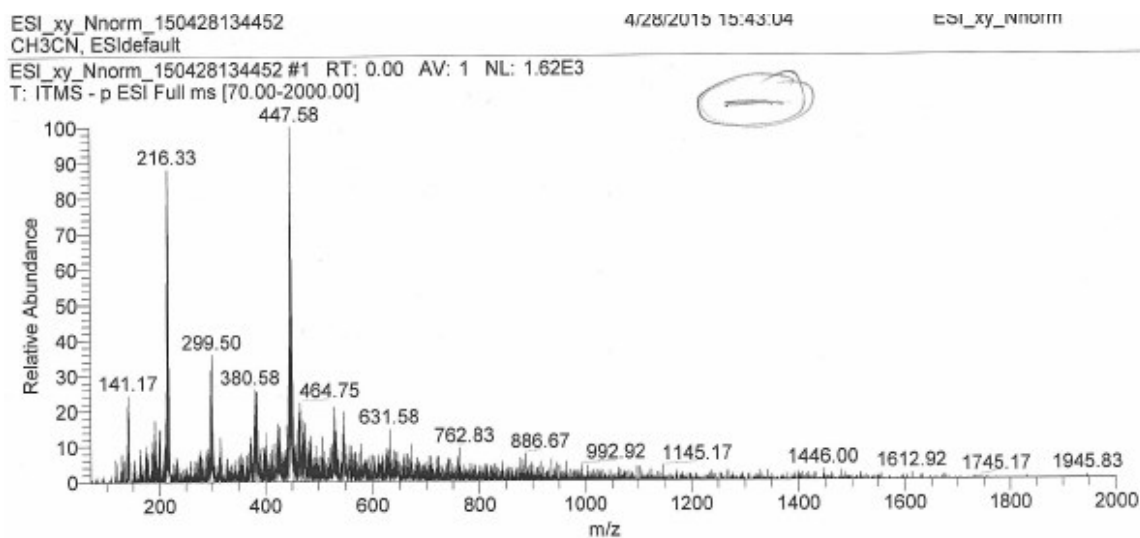


Figure S17. Reference (left-hand side) and 270 minute irradiated (right-hand side) samples of *anti*-B₁₈H₂₂ in *c*-hexane under UV lamp irradiation.

